Mass perturbation of a body segment: 1. Effects on segment dynamics

van Soest, A.J.; Peper, C.E.; Selles, R.W.

published in
Journal of Motor Behavior
2004

DOI (link to publisher)
10.3200/JMBR.36.4.419-424

document version
Publisher's PDF, also known as Version of record

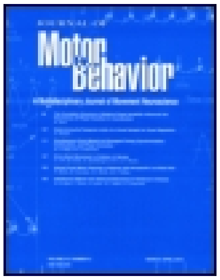

Journal of Motor Behavior
Publication details, including instructions for authors and subscription information:
http://www.tandfonline.com/loi/vjmb20

Mass Perturbation of a Body Segment: I. Effects on Segment Dynamics

A. J. (Knoek) van Soest [a] , C. (Lieke) E. Peper [b] & R. (Ruud) W. Selles [c]

[a] Institute for Fundamental and Clinical Human Movement Sciences Amsterdam/Nijmegen

[b] Vrije Universiteit Faculty of Human Movement Sciences Amsterdam, The Netherlands

[c] Department of Rehabilitation Medicine Erasmus Medical Center Rotterdam The Netherlands

Version of record first published: 07 Aug 2010.

To cite this article: A. J. (Knoek) van Soest, C. (Lieke) E. Peper & R. (Ruud) W. Selles (2004): Mass Perturbation of a Body Segment: I. Effects on Segment Dynamics, Journal of Motor Behavior, 36:4, 419-424

To link to this article: http://dx.doi.org/10.3200/JMBR.36.4.419-424

Journal of Motor Behavior, 2004, Vol. 36, No. 4, 419–424

Mass Perturbation of a Body Segment: I. Effects on Segment Dynamics

A. J. (Knoek) van Soest
C. (Lieke) E. Peper
Institute for Fundamental and Clinical Human Movement Sciences
Amsterdam/Nijmegen, and
Faculty of Human Movement Sciences
Vrije Universiteit, Amsterdam, The Netherlands

R. (Ruud) W. Selles
Department of Rehabilitation Medicine
Erasmus Medical Center
Rotterdam, The Netherlands

ABSTRACT. Investigators often use mass perturbation of body segments as an experimental paradigm to study movement coordination. To analyze the effect of mass perturbation on small-amplitude oscillations, the authors linearize the equation of motion of a single segment moving in a vertical plane and derive the effect of added mass on the undamped eigenfrequency, the relative damping, and the low-frequency control gain of the segment. Mass addition results in a decrease in both the relative damping and the low-frequency control gain; the undamped eigenfrequency increases for mass addition between the pivot point and R_0 (where R_0 is the length of a point mass pendulum whose undamped eigenfrequency is identical to that of the unperturbed segment), decreases for mass addition beyond R_0, and remains unaffected for mass addition at R_0. For a typical lower leg + foot segment, R_0 is just proximal to the ankle joint. That location may explain the absence of an effect on oscillation frequency in studies in which mass has been added to the ankle. The authors' analysis provides a basis for a more effective application of mass perturbations in future experiments.

Key words: dynamics, eigenfrequency, mass perturbation, segment inertia

Control of periodic movements, such as gait, is facilitated by exploiting the undriven dynamics of the skeletal system; when a limb is moved at (or close to) its eigenfrequency, the mechanical oscillator may take care of (part of) the control problem (e.g., McGeer, 1993; Taga, Yamaguchi, & Shimizu, 1991; Van der Linde, 1999). Assuming that movement coordination builds on the undriven dynamics, one way researchers can gain insight into movement coordination is through perturbation of the undriven dynamics of the mechanical system. Limb mass, a parameter that affects the mechanical behavior of the limb, lends itself easily to experimental manipulation. In this study, we use the term *mass perturbation* for situations in which mass is semipermanently attached to a body segment; thus, wearing heavy boots is a real-world example of a mass perturbation. In studies on prosthetic design (for a review, see Selles, Bussmann, Wagenaar, & Stam, 1999), investigators have used mass perturbations to influence the undriven oscillatory dynamics of the mass-perturbed limb and, therefore, the walking pattern. A key issue in several prosthetic design studies has been to identify the inertial properties of the prosthesis that allow the swing phase in gait to be nearly passive. In coordination dynamics studies (e.g., Jeka & Kelso, 1995), investigators have perturbed mass so that they could examine how the resulting changes in the undriven oscillation frequencies affect the coordination between mechanically independent limbs.

Even for the simplest conceivable case, that is, for a single undriven rigid limb segment rotating about a fixed axis in the absence of damping, it is not immediately clear how the magnitude and location of the added mass affect the oscillatory dynamics. On the one hand, adding mass increases the gravitational stiffness, defined as the change in gravitational torque per change in joint angle. By itself, that increase in gravitational stiffness tends to increase the undriven oscillation frequency. At the same time, however, adding mass increases the moment of inertia of the limb (relative to the joint axis), which by itself tends to decrease the undriven oscillation frequency. In this article, we analyze the net result of those opposed effects of mass perturbation. In particular, we analyze the effects of magnitude and location of added mass on the small-amplitude dynamics of a limb segment, in terms of its effect on the parameters of the linearized system: the undamped and damped eigenfrequencies, the relative damping, and the low-frequency control

Correspondence address: A. J. van Soest, Faculty of Human Movement Sciences, Vrije Universiteit, Van der Boechorststraat 9, 1081 BT Amsterdam, The Netherlands. E-mail address: a_j_van_soest@fbw.vu.nl

gain. In addition, we assess the applicability of the results to the large-amplitude case. The results may help researchers to base mass perturbations on sound mechanical grounds in future studies.

Method

Nonlinear Equation of Motion

Our analysis is restricted to a system that comprises a single rigid limb segment rotating around a fixed pivot point p in a two-dimensional vertical plane. Most of the segment parameters are defined in Figure 1. The moment of inertia of the unperturbed segment is described by its radius of gyration R_{gyr} relative to p (where, by definition, the unperturbed moment of inertia relative to p equals $m \cdot R^2_{\text{gyr}}$). The forces and net torques acting on that segment are also shown in Figure 1. The rotational effect of the force of gravity is represented by T_G, the gravitational torque relative to the pivot point p. The net joint torque T_p represents the net mechanical effect of both the passive (e.g., ligaments) and the active (i.e., muscles) structures that may produce torques relative to the joint axis. Thus, T_p is assumed to be a function of angle, angular velocity (capturing the viscoelastic part of the torque produced by both passive and active structures), and an independent input T_{act} (which captures the active part of the muscle torque that results from the neural drive to the muscles). For a segment perturbed by a mass Δm at distance R from the pivot point, the rotational equation of motion relative to p is

$$T_G(\varphi) + T_p(\varphi, \dot{\varphi}; T_{\text{act}}) = I_p \cdot \ddot{\varphi}, \tag{1}$$

where (taking g positive)

$$T_G = -(m \cdot R_{\text{cm}} + \Delta m \cdot \mathrm{R}) \cdot g \cdot \sin(\varphi), \tag{2a}$$

and

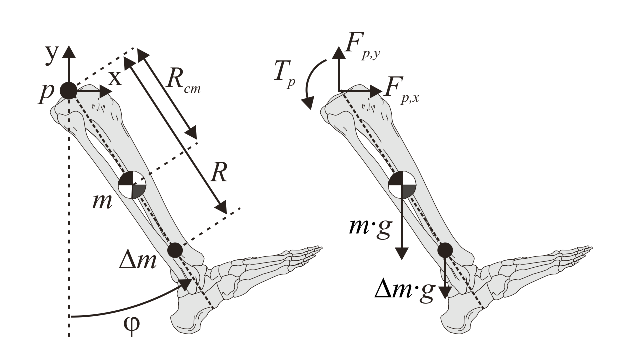

FIGURE 1. Left. The parameters used to describe the segment and the mass perturbation. Point p is the pivot point, R_{cm} is the distance from p to the segment mass center, m is the segment mass; R is the distance from p to the added point mass, and Δm is the magnitude of the added mass. **Right.** The forces and torques acting on the segment; note that the joint reaction forces do not appear in Equation 1 because point p was used as the point of rotation.

$$I_p = (m \cdot R^2_{\text{gyr}} + \Delta m \cdot R^2). \tag{2b}$$

One can obtain the equation of motion for the unperturbed segment by setting $\Delta m = 0$.

In the absence of damping and driving (i.e., when $T_p = 0$), the dynamics of this nonlinear second-order system is completely understood (e.g., Strogatz, 1994). Yet, because of the nonlinearity of Equation 1, an analytical derivation of the effect of Δm and R is impossible in the more general case ($T_p \neq 0$). Therefore, in the present article we assess the effect of mass perturbation in the context of linearizations of Equation 1, that is, for small-amplitude oscillations about a linearization point.

Linearized Equation of Motion

Linearization (first-order Taylor approximation) of Equation 1 about any point $\varphi = \varphi^{\#}, \dot{\varphi} = \dot{\varphi}^{\#}, T_{\text{act}} = T^{\#}_{\text{act}}$ yields an instantiation of the following equation:

$$\left.\frac{\partial T_G}{\partial \varphi}\right|_{\varphi=\varphi^{\#}} \cdot \Delta\varphi + \left.\frac{\partial T_p}{\partial \varphi}\right|_{\substack{\varphi=\varphi^{\#}\\ \dot{\varphi}=\dot{\varphi}^{\#}\\ T_{\text{act}}=T^{\#}_{\text{act}}}} \cdot \Delta\varphi + \left.\frac{\partial T_p}{\partial \dot{\varphi}}\right|_{\substack{\varphi=\varphi^{\#}\\ \dot{\varphi}=\dot{\varphi}^{\#}\\ T_{\text{act}}=T^{\#}_{\text{act}}}} \cdot \Delta\dot{\varphi} + \left.\frac{\partial T_p}{\partial T_{\text{act}}}\right|_{\substack{\varphi=\varphi^{\#}\\ \dot{\varphi}=\dot{\varphi}^{\#}\\ T_{\text{act}}=T^{\#}_{\text{act}}}} \cdot \Delta T_{\text{act}} = I \cdot \Delta\ddot{\varphi} \tag{3}$$

For any of the variables *var* involved, Δ*var* in that equation refers to the change in *var* relative to the linearization point. We define the joint rotational stiffness $K_{T_p} = -\partial T_p/\partial\varphi$ and the joint rotational damping $B_{T_p} = -\partial T_p/\partial\dot{\varphi}$ to simplify notation, so that K_{T_p} and B_{T_p} capture the elastic and viscous contribution of both passive structures and muscles to T_p. Using those definitions, and after working out the term concerning the gravitational torque T_G (cf. Equation 2a), we obtain the following after some rearrangement:

$$(m \cdot R^2_{\text{gyr}} + \Delta m \cdot R^2) \cdot \Delta\ddot{\varphi} + B_{Tp} \cdot \Delta\dot{\varphi} + [(m \cdot R_{\text{cm}} + \Delta m \cdot R) \cdot g \cdot \cos(\varphi^{\#}) + K_{Tp}] \cdot \Delta\varphi = \Delta T_{\text{act}} \tag{4}$$

To characterize the linearized system in terms of standard parameters, we relate Equation 4 (see Results section) to the following standard form for the equation of motion of a linear second-order ordinary differential equation:

$$\frac{1}{\omega_0^2} \cdot \Delta\ddot{\varphi} + \frac{2\beta}{\omega_0}\Delta\dot{\varphi} + \Delta\varphi = k_{\text{act}} \cdot \Delta T_{\text{act}}. \tag{5}$$

Here, k_{act} is the low-frequency control gain—the steady state value of $\Delta\varphi$ for a unity value in the input ΔT_{act}. β is the relative damping: $\beta = 0$ indicates an undamped system,

$\beta = 1$ indicates critical damping, and $\beta > 1$ indicates that the system does not oscillate. Last, ω_0 is the undamped eigenfrequency—the angular frequency of the sinusoidal oscillations that occur in the absence of input and when $\beta = 0$. The directly observable oscillation frequency ω_n of the damped system, which is also referred to as the *damped eigenfrequency*, is a function of ω_0 and β: $\omega_n = (1 - \beta^2)^{0.5} \cdot \omega_0$.

Results

Effect of Mass Perturbation on Linear System Parameters: Small-Amplitude Case

One can find the linear system's parameters as a function of Δm and R by relating Equation 4 to Equation 5, with the following result:

$$\omega_0(R,\Delta m) = \sqrt{\frac{g \cdot \cos(\varphi^{\#}) \cdot (m \cdot R_{\mathrm{cm}} + \Delta m \cdot R) + K_{T_p}}{m \cdot R_{\mathrm{gyr}}^2 + \Delta m \cdot R^2}}. \qquad (6)$$

The term $g \cdot \cos(\varphi^{\#}) \cdot (m \cdot R_{\mathrm{cm}} + \Delta m \cdot R)$ in Equation 6 represents the gravitational stiffness, for which we use the symbol K_G in Equations 7 and 8.

$$\beta(R,\Delta m) = \frac{B_{Tp}}{2 \cdot \sqrt{(K_G + K_{Tp}) \cdot (m \cdot R_{\mathrm{gyr}}^2 + \Delta m \cdot R^2)}}. \qquad (7)$$

$$k_{\mathrm{act}}(R,\Delta m) = \frac{1}{K_G + K_{Tp}}. \qquad (8)$$

Substitution of $\Delta m = 0$ in those equations yields the reference values $\omega_{0,\mathrm{ref}}, \beta_{\mathrm{ref}}, k_{\mathrm{act,ref}}$ associated with the unperturbed segment.

Inspection of Equations 7 and 8 reveals that both relative damping and low-frequency control gain become smaller for any mass addition Δm at any location R. The effect of mass addition on the undamped eigenfrequency ω_0 (Equation 6) is less straightforward. The presence of a linear term in R in the numerator and a quadratic term in R in the denominator indicates that a value of R must exist for which $\omega_0 = \omega_{0,\mathrm{ref}}$, irrespective of the value of Δm. That value of R, which we refer to as R_0, can be interpreted as the length of a point mass pendulum for which ω_0 is equal to that of the unperturbed body segment. An expression for R_0 is easily found:

$$R_0 = \frac{R_{\mathrm{gyr}}^2}{R_{\mathrm{cm}} + \dfrac{K_{Tp}}{m \cdot g \cdot \cos(\varphi^{\#})}}. \qquad (9)$$

By combining Equation 9 with Equation 6, the following helpful expression can be derived for ω_0 relative to $\omega_{0,\mathrm{ref}}$:

$$\omega_0(R,\Delta m) = \omega_{0,\mathrm{ref}} \cdot \sqrt{\frac{\left(R_{\mathrm{cm}} + \dfrac{K_{Tp}}{m \cdot g \cdot \cos(\varphi^{\#})}\right)^2 + R_{\mathrm{gyr}}^2 \cdot \dfrac{\Delta m}{m} \cdot \dfrac{R}{R_0}}{\left(R_{\mathrm{cm}} + \dfrac{K_{Tp}}{m \cdot g \cdot \cos(\varphi^{\#})}\right)^2 + R_{\mathrm{gyr}}^2 \cdot \dfrac{\Delta m}{m} \cdot \dfrac{R^2}{R_0^2}}}. \qquad (10)$$

From Equation 10, one can see more directly that (a) mass addition at $R = 0$ or at $R = R_0$ does not affect the undamped eigenfrequency, (i.e., $\omega_0 = \omega_{0,\mathrm{ref}}$), (b) mass addition for which $0 < R < R_0$ results in an increase in ω_0 (i.e., $\omega_0 > \omega_{0,\mathrm{ref}}$) and (c) that mass addition at $R > R_0$ leads to a decrease in ω_0 (i.e., $\omega_0 < \omega_{0,\mathrm{ref}}$).

Similarly, the equations that express the effect of Δm and R on β and k_{act} relative to the reference values of those parameters can be found:

$$\beta(R,\Delta m) / \beta_{\mathrm{ref}} = \sqrt{\frac{\left(R_{\mathrm{cm}} + \dfrac{K_{Tp}}{m \cdot g \cdot \cos(\varphi^{\#})}\right) \cdot R_{\mathrm{gyr}}^2}{\left(\left(R_{\mathrm{cm}} + \dfrac{K_{Tp}}{m \cdot g \cdot \cos(\varphi^{\#})}\right) + \dfrac{\Delta m}{m} \cdot R\right) \cdot \left(R_{\mathrm{gyr}}^2 + \dfrac{\Delta m}{m} \cdot R^2\right)}}. \qquad (11)$$

$$k_{\mathrm{act}}(R,\Delta m) = k_{\mathrm{act,ref}} \cdot \frac{\left(R_{\mathrm{cm}} + \dfrac{K_{Tp}}{m \cdot g \cdot \cos(\varphi^{\#})}\right)}{\left(R_{\mathrm{cm}} + \dfrac{K_{Tp}}{m \cdot g \cdot \cos(\varphi^{\#})}\right) + \dfrac{\Delta m}{m} \cdot R}. \qquad (12)$$

As an example, consider the situation $\varphi^{\#} = \dot{\varphi}^{\#} = T_{\mathrm{act}} = 0$, representing passive swinging. Parameter values for the unperturbed situation have been derived from a single-participant experiment, involving passive swinging of the lower leg + foot segment (see Appendix). Using the estimated values for that participant for the joint rotational stiffness and damping K_{Tp} and B_{Tp}, which result in $\omega_{0,\mathrm{ref}} = 5.68\ \mathrm{rad} \cdot \mathrm{s}^{-1}$, $\beta_{\mathrm{ref}} = 0.08$, and $k_{\mathrm{act,ref}} = 0.08\ \mathrm{rad} \cdot (\mathrm{N} \cdot \mathrm{m})^{-1}$, the effect of Δm and R on ω_0, β, and k_{act} of the lower leg + foot segment as predicted from Equations 6–8 is illustrated in Figure 2. In addition, the effect on the damped eigenfrequency ω_n (which depends on ω_0 and β; see Method) is presented.

Large-Amplitude Oscillation

A direct comparison between the linear small-amplitude case just discussed and the nonlinear large-amplitude case is complicated by the fact that the standard parameters for the linear system have no straightforward counterparts in the nonlinear system. In fact, the only parameters that can be compared are the oscillation frequencies of the undamped and damped systems. To investigate the effect of

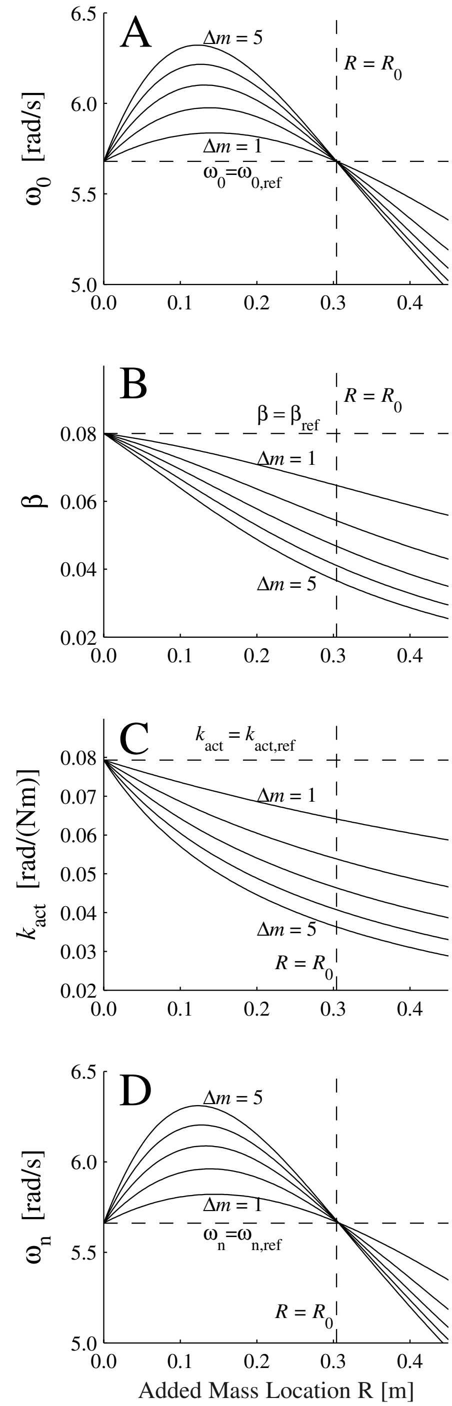

FIGURE 2. Effects of added mass Δm and distance R as predicted from Equations 6–8 on (**A**) the undamped eigenfrequency ω_0, (**B**) the dimensionless relative damping β, (**C**) the low-frequency control gain k_{act}, and (**D**) the damped eigenfrequency ω_n, all for the lower leg + foot segment of the male participant in the experiment described in the Appendix (segment length = 0.41 m, m = 4.2 kg, R_{cm} = 0.250 m, and R_{gyr} = 0.303 m, resulting in R_0 = 0.304 m, K_{Tp} = 2.19 Nm · rad^{-1} and B_{Tp} = 0.35 N · m · s · rad^{-1}). The pivot point (knee axis of rotation) was assumed to be fixed. Separate curves are for Δm = 1, 2, 3, 4, and 5 kg. See Method section for definitions.

mass perturbation on the damped oscillation frequency, we considered the following instantiation of Equation 1:

$$-(m \cdot R_{cm} + \Delta m \cdot R) \cdot g \cdot \sin(\varphi) - K_{Tp} \cdot \varphi - B_{Tp} \cdot \dot{\varphi} = I_p \cdot \ddot{\varphi} \quad (13)$$

That is, we took into account the nonlinearity in the gravitational torque, whereas we assumed that the joint torque depended linearly on joint angle and angular velocity. We obtained particular solutions of that equation of motion through simulation for a range of oscillation amplitudes (i.e., a range of initial deflections) for a 1-kg mass perturbation at variable R. Damped oscillation frequencies as determined from the simulation results are presented in Figure 3.

Discussion

Using linear approximations, we analyzed the effect of mass perturbation on the parameters of a body segment rotating about a fixed pivot point under the influence of gravity. We found that the relative damping and the low-frequency control gain are reduced by mass addition (see Figures 2B and 2C). The gain reduction implies that equilibrium (i.e., $\Delta\dot{\varphi} = \Delta\ddot{\varphi} = 0$ at any $\Delta\varphi$) requires a larger net joint torque in the presence of added mass. The reduction of the relative damping implies that more oscillations will take place during relaxation. That implication can be understood from the fact that the same mechanical joint rotational damping B_{Tp} now acts on a segment with increased total

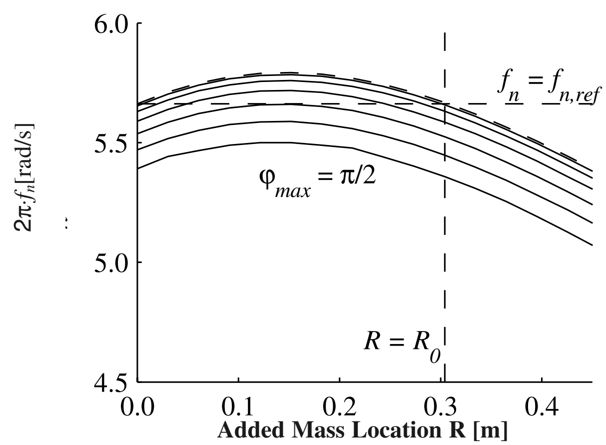

FIGURE 3. Effect of oscillation amplitude (initial deflection of the lower leg+foot segment) on the relation between distance R and the damped oscillation frequency f_n, for an added mass of 1 kg, as estimated from simulation of Equation 13. To allow for easy comparison with Figure 2D, we plotted $2\pi \cdot f_n$ rather than f_n itself. Dashed curve is for the linearized model (i.e., initial deflection $\varphi_{max} \approx 0$). Solid curves are for initial deflections φ_{max} of $\pi/12$, $2\pi/12$, $3\pi/12$, $4\pi/12$, $5\pi/12$, and $6\pi/12$ rad. $f_{n,ref}$ reflects f_n for the linear model in the absence of mass perturbation, that is, $2\pi \cdot f_{n,ref} = \omega_{n,ref}$. Note that for each oscillation amplitude, f_n for $R = 0$ was identical to f_n for the unperterbed segment. Parameter values are identical to those used in Figure 2.

stiffness (i.e., the coefficient of $\Delta\varphi$ in Equation 4) and total inertia (i.e., the coefficient of $\Delta\ddot{\varphi}$ in Equation 4).

The most interesting result concerns the effect of mass addition on the undamped eigenfrequency ω_0. Mass addition at a distance R_0 from the pivot point (R_0 being the length of a point mass pendulum for which ω_0 is equal to that of the unperturbed body segment; see Equation 9), is found not to affect ω_0. That finding reflects the basic fact that ω_0 of a point mass pendulum is independent of mass magnitude, which implies that adding mass to a body segment at a distance from the pivot point that is equal to the length of the equivalent point mass pendulum does not affect ω_0. All in all, the relation between R and ω_0 is found to be nonmonotonous (see Figure 2A): When mass is added between the pivot point and R_0, ω_0 increases; for mass addition beyond R_0, ω_0 decreases. Qualitatively, those nonmonotonic changes in ω_0 (see Figure 2A) can be readily appreciated from the fact that for any second-order mechanical system (cf. Equations 4–5), ω_0 is determined by the ratio of the effective stiffness (i.e., the coefficient of $\Delta\varphi$ in Equation 4) over the effective inertia (i.e., the coefficient of $\Delta\ddot{\varphi}$ in Equation 4). The contribution of mass addition to the stiffness is linearly related to R, whereas its contribution to inertia is quadratically related to R (see Equation 6). As a result, the increase in stiffness dominates at $0 < R < R_0$, resulting in an increased ω_0. In contrast, the increase in inertia dominates at $R > R_0$, resulting in a decreased ω_0. Finally, the effect of mass addition on ω_n, the damped eigenfrequency, can be reconstructed from the effects on both ω_0 and β; given the fact that β was found to be very low during passive swinging ($\beta_{ref} = 0.08$), it is not surprising that the results for ω_n were almost indistinguishable from those for ω_0 (cf. Figures 2A and D). It should be kept in mind, however, that for an oscillating system with substantial damping (i.e., $0.5 < \beta < 1$), the results for ω_n will deviate from those for ω_0 (data not shown).

In passing, we would like to point out that the equations pertaining to the linearized system are more generally applicable than has been shown so far. First of all, Equations 10–12 are completely valid when linearization is performed around an equilibrium at any angle $\varphi \neq 0$. Second, those equations are valid when the pivot point is not fixed in space, as long as its kinematics is prescribed as a function of time. Finally, the system can be linearized about a trajectory, yielding a second-order system with time varying parameters $\omega_0(t)$, $\beta(t)$, and $k_{act}(t)$. Those parameters formally describe the dynamical response to small perturbations of the reference trajectory, even though interpretation is difficult because of the time dependency. Again, Equations 10–12 capture the effect of mass perturbation on the values of those parameters.[1]

It is well known that (and how) the oscillation frequency of an undamped undriven pendulum decreases monotonically with oscillation amplitude (Young & Freedman, 1996). Thus, it is obvious that $\omega_{0,ref}$ and β_{ref}, as obtained through linearization, would not provide an accurate prediction of the large-amplitude damped oscillation frequency (see Figure 3). However, for the low damping case considered, the changes in the damped eigenfrequency induced by mass perturbations were virtually independent of oscillation amplitude (see Figure 3); in other words, when there is little damping, one can use Equations 10–11 to predict the mass-perturbation-induced change in damped oscillation frequency of large-amplitude oscillation.

In gait studies, investigators have typically added mass just proximal to the ankle joint of a normal (e.g., Donker, Mulder, Nienhuis, & Duysens, 2002; Skinner & Barrack, 1990) or prosthetic (e.g., Tashman, Hicks, & Jendrzejczyk, 1985) leg, in an attempt to decrease ω_0. In the three mentioned studies, the authors found a negligible effect on the step frequency. The present analysis indicates that the chosen point, just proximal to the ankle, is close to R_0 of the lower leg + foot segment (see Figure 2A). As a result, the obtained negligible effect is in agreement with our model. If substantial slowing is to be achieved, one should add mass at a distance that exceeds segment length (which may be problematic in practice).

A similar caveat applies to studies regarding the relation between eigenfrequency differences and relative phasing in the coordination between two nonhomologous limb segments. To achieve comparable eigenfrequencies between the forearm + hand and the lower leg + foot, one may decrease the eigenfrequency of the forearm + hand by means of a mass perturbation. Because the segment properties of the forearm + hand (Plagenhoef, Evans, & Abdelnour, 1983) are such that R_0 is close to the wrist joint, adding a mass close to that position (e.g., Serrien & Swinnen, 1998) will not effectuate the desired experimental manipulation. In fact, the present results suggest that it may be more practical to increase the eigenfrequency of the slower segment (i.e., lower leg + foot) by adding mass at $0 < R < R_0$ than to decrease that of the faster segment (i.e., forearm + hand), which requires $R > R_0$.

In conclusion, on the basis of a linearized model, we have derived equations from which the effect of mass perturbation on segment dynamics can be estimated. Furthermore, our simulation results suggest that the analytical expressions relating to the linear case are also helpful when the large-amplitude, nonlinear case is considered. As such, the analysis presented in this article may be a helpful tool in the design of future mass-perturbation studies, as exemplified in the accompanying article (Peper, Nooij, & van Soest, 2004).

ACKNOWLEDGMENT

We gratefully acknowledge the assistance of Wamima in carrying out the experiment. The contribution of Lieke Peper was facilitated by ASPASIA Grant 015.001.040 of the Netherlands Organization for Applied Scientific Research (NWO).

NOTE

1. In deriving Equations 10–12, we assumed that the joint stiffness K_{Tp} and the joint damping B_{Tp} are not affected by the mass perturbation. In general, however, K_{Tp} and B_{Tp} are a function of the muscle-generated net joint torque T_p. Thus, that assumption may be violated in applications in which mass perturbation results in a

substantial change in net joint torque, which may render Equations 10–12 inadequate in such situations.

REFERENCES

Donker, S. F., Mulder, T., Nienhuis, B., & Duysens, J. (2002). Adaptations in arm movements for added mass to wrist or ankle during walking. *Experimental Brain Research, 146,* 26–31.

Jeka, J. J., & Kelso, J. A. S. (1995). Manipulating symmetry in the coordination dynamics of human movement. *Journal of Experimental Psychology: Human Perception and Performance, 21,* 360–374.

McGeer, T. (1993). Dynamics and control of bipedal locomotion. *Journal of Theoretical Biology, 163,* 277–314.

Peper, C. E., Nooij, S. A. E., & van Soest, A. J. (2004). Mass perturbation of a body segment: 2. Effects on interlimb coordination. *Journal of Motor Behavior, 36*, 425–441.

Plagenhoef, S., Evans, F. G., & Abdelnour, T. (1983). Anatomical data for analyzing human motion. *Research Quarterly for Exercise and Sport, 54,* 169–178.

Selles, R. W., Bussmann, J. B. J., Wagenaar, R. C., & Stam, H. J. (1999). Effects of prosthetic mass and mass distribution on kinematics and energetics of prosthetic gait: A systematic review. *Archives of Physical Medicine and Rehabilitation, 80,* 1593–1599.

Serrien, D. J., & Swinnen, S. P. (1998). Load compensation during homologous and non-homologous coordination. *Experimental Brain Research, 121,* 223–229.

Skinner, H. B., & Barrack, R. L. (1990). Ankle weighting effect on gait in able-bodied adults. *Archives of Physical Medicine and Rehabilitation, 71,* 112–115.

Strogatz, S. H. (1994). *Nonlinear dynamics and chaos*. Reading MA: Perseus Books.

Taga, G., Yamaguchi, Y., & Shimizu, H. (1991). Self-organized control of bipedal locomotion by neural oscillators in unpredictable environment. *Biological Cybernetics, 65,* 147–159.

Tashman, S., Hicks, R. R., & Jendrzejczyk, D. R. (1985). Evaluation of a prosthetic shank with variable inertial properties. *Clinical Prosthetics and Orthotics, 9,* 23–28.

Van der Linde, R. Q. (1999). Passive bipedal walking with phasic muscle contraction. *BiologicalCybernetics, 81,* 227–237.

Young, H. D., & Freedman, R. A. (1996). *University physics*. Reading, MA: Addison Wesley.

APPENDIX

Parameter Values for the Unperturbed Lower Leg + Foot Segment

We performed a single-participant experiment in which our sole objective was to obtain parameter values for an unperturbed, male, lower leg + foot segment swinging passively around a fixed knee axis. In the experiment, the barefoot participant was seated on a horizontal surface. Active markers were attached to the lateral epicondylus and to the distal tip of the lateral malleolus of the right leg. The participant was instructed to relax completely. Subsequently, the experimenter deflected the right lower leg + foot segment from the freely hanging equilibrium position by approximately 0.3 rad, and released it. Using an Optotrak system (Northern Digital, Inc., Waterloo, Ontario, Canada), we tracked the positions of the two markers at a sampling frequency of 100 Hz during the subsequent passive relaxation. We calculated the deflection angle φ from the marker coordinates, without any filtering of the data.

Characteristics of the healthy male participant were age = 24 years, body length = 1.785 m, body weight = 68.7 kg, and lower leg length = 0.41 m. From those characteristics, and following Plagenhoef et al. (1983), we estimated the mass of the lower leg + foot at 4.2 kg, R_{cm} (the distance from pivot point p to the segment mass center) was estimated at 0.250 m, and R_{gyr} was estimated at 0.303 m. A second-order model was least squares fitted to the $\varphi(t)$ data. As expected, the model fit the data closely (Pearson's r = .99). The least squares fit resulted in K_{Tp} = 2.19 $\mathrm{N \cdot m \cdot rad^{-1}}$ and B_{Tp} = 0.35 $\mathrm{N \cdot m \cdot s \cdot rad^{-1}}$; note that any errors in gravitational stiffness that result from errors in the estimated inertial parameters are compensated in the value of K_{Tp}. After substitution of those values into Equations 6–8, we found $\omega_{0,\mathrm{ref}}$ = 5.68 $\mathrm{rad \cdot s^{-1}}$, β_{ref} = 0.08, and $k_{\mathrm{act,ref}}$ = 0.08 $\mathrm{rad \cdot (N \cdot m)^{-1}}$ for the participant in our experiment.

Submitted January 7, 2003
Revised May 7, 2003